agronomy

MDPI

Article

Continuous Field Monitoring of Growth and Thickness Variation in a Potato Tuber Using a Strain-Gauge Sensor

Steven O. Link

Link Agricultural Technologies LLC., West Richland, WA 99353, USA; stevenlink@me.com

Abstract

Real-time measurement of belowground tuber growth has not been conducted in field crops. Here, a strain-gauge sensor was used to monitor the growth of a single potato tuber and estimate its daily water loss. Over the 11 days preceding harvest, tuber thickness increased by 0.80 mm, corresponding to a daily gain of 1.4 g, or a 4.2% increase. The greatest diurnal fluctuation was 0.439 mm, corresponding to a transpirational water loss of 9.1 mL, or 2.9% of the tuber's water content. Daily estimated transpiration showed a positive correlation with estimated vapor pressure deficit. This sensor may enable more precise input control and higher temporal resolution than current methods for below-ground crops, supporting improved crop management, yield prediction, and harvest decisions.

Keywords: phenotyping; dendrometer; agriculture; electronic instrumentation; tubers; signal processing; growth; water status

1. Introduction

Measuring plants and their edible parts is crucial for understanding and managing plant growth. Efficient growth management involves adjusting resource inputs, such as water and nutrients, to maximize yield and quality while minimizing resource use. For managing aboveground crops, some workers now use real-time assessments of plant and fruit growth with dendrometers and fruit sensors to keep growth at target levels [1]. While this method is fairly straightforward for aboveground tissues, it becomes much more difficult for belowground tissues because soil can interfere with mechanical sensors like dendrometers [2]. To address this problem, Ref. [2] use a complex magnetic resonance imaging (MRI) tool to monitor tuber growth and water content, but only every four hours over four days. Unfortunately, MRI is not suitable for fieldwork. An alternative method is needed.

Others [3,4] measure changes in the size of *Solanum tuberosum* L. tubers underground in greenhouse and laboratory settings, but the technology remains too fragile or complex for field use. An effort has also been made to measure potato tubers in real time in field conditions. A linear variable differential transformer (LVDT) for field trials is used on a nearly fully exposed potato after the soil is removed [5]. This was done to avoid soil interference, but it may bias the tuber response relative to that of buried tubers. Additionally, they use a narrow, curved tube to house a wire transmitting length changes to the LVDT, but the wire touches the tube's surface, thereby interfering with the signal as the potato shrinks during the day. The authors note that a better design is needed. A reliable, field-tested sensor is used on apples [6,7], tomatoes [8], cherries [9], cucumbers [10], and olives [11] to measure growth, and is the focus of this study.

Academic Editor: Jian Zhang

Received: 10 July 2026
Revised: 2 September 2026
Accepted: 7 September 2026
Published: 14 September 2026

This sensor and other similar sensors also monitor water status by detecting very small diurnal changes in thickness, indicating water gain at night and loss during the day [12]. Diurnal variation in thickness is linked to plant water potential in stems [8,12,13], to relative water content in fruit [14], and to transpiration [15–17]. It should be noted that below-ground potato tubers are thickened stem-storage tissues that form at the ends of stolons and can store large amounts of water. For example, 82% of a Shepody cultivar tuber is water [18]. Given the large volume of water stored in tubers, it is important to determine how much of this water contributes to the plant's overall transpiration for water budgeting. As [2] note, little is known about water fluxes into and out of tubers because measuring such fluxes below ground is challenging. In a controlled greenhouse study using MRI, they find that in 6-week-old well-watered plants, about 10% of the water in tubers is lost during the day and transferred to the plant's vegetative parts for transpiration. No further information is available about this process. Here, the amount of water lost by the test tuber was estimated, with the expectation that it may lose less water toward the end of the vegetative growth cycle as leaves begin to senesce. Additionally, since the vegetative part of potato plants shows a typical positive correlation between transpiration and vapor pressure deficit (VPD) for well-watered plants [19,20], it is hypothesized that there will be a positive correlation between daily shrinkage or water loss in a tuber and mean daily VPD.

This study aimed to determine whether the device could adequately monitor real-time changes in below-ground tuber size in an agricultural setting. Testing was conducted to (i) determine whether the device can accurately measure underground tuber growth and daily changes in thickness; (ii) determine whether, after separating the long-term growth signal from diurnal variation, the resulting assessment of water status can be used to quantify the amount of water lost during the day; and (iii) determine whether the daily water loss rate or the tuber's contribution to transpiration can be related to daily vapor pressure deficit. These highly sensitive strain gauges can produce outliers or spikes due to electrical noise from motors [21], soil vibrations from the regular movement of pivot irrigation systems [22], and possibly water leakage through the sensor seals [23]. A soil moisture sensor was installed to monitor potential impacts of pivot irrigation on the signal. Removing spikes from strain gauge data is typically done using a moving median filter with a fixed threshold [24]. Given that this is a proof-of-concept study with only one sensor, there is no suggestion that the results are representative of other potatoes. Comparisons with other studies and possible uses of the information are presented to suggest future uses of the technology.

2. Materials and Methods

2.1. Field Propagation

The study was carried out on a 51-acre irrigated crop circle just north of Pasco, WA (46.37027957, −119.13218795; elevation: 201.8 m). The soil consisted of Quincy loamy fine sand. The potato variety used was Shepody, which was seeded in early March. Data collection was conducted from 9 July to 22 July 2025, until harvest.

2.2. Sensor

The sensor [6] (Dynamax, Inc., Houston, TX, USA) consists of two aluminum bars, each 76.2 mm long, attached to a flexible stainless-steel band with strain gauges mounted on it (Figure 1A). The flexible stainless-steel band is 152.4 mm long, 25.4 mm wide, and 0.76 mm thick. The four strain gauges are connected in a full Wheatstone bridge configuration, with two gauges on each side positioned at the center of the band. The sensor was secured to the tuber by tightening a bolt with a curved anvil at its end, threaded through one of the aluminum bars, and pressing the potato between two anvils (Figure 1A,B). Part of the sensor and the potato were covered by soil, except where blocked by a black pipe

(Figure 1C). The pipe was oriented north to minimize light exposure. A platinum resistance thermometer (PRT) sensor was placed at the junction of the spring-steel band and the nearby aluminum bar, but not in the soil. The Delta-T soil moisture sensor was positioned horizontally in the soil at the same depth as the tubers. The soil moisture sensor was then covered with soil and tightly packed.

Figure 1. Tuber sensor and field implementation. (**A**) The strain gauge C-clamp [6] model DEX100 (Dynamax Inc., Houston, TX, USA) on a potato tuber. (**B**) The sensor was placed on the cleaned upper surface of the tuber. The metal anvil contacts the cleaned tuber and is inserted through an approximately 3 cm long black plastic pipe, flush with the tuber surface, pointing north. (**C**) The sensor on the buried tuber, except where the soil was blocked by the black plastic pipe. The square metal anvil is touching the potato inside the pipe, as shown in Figure 1A, and is positioned to measure the height dimension. (**D**) The equipment (Dynamax, Inc.) set up on 9 July included a solar panel, a 12-volt deep-cycle battery, an air temperature sensor inside the white acrylonitrile butadiene styrene (ABS) plastic data logger housing, and a data logger with a transmitter mounted on a tripod.

As the tuber thickness varied, the differences in the relative tension experienced by the strain gauges were recorded as voltage signals. The strain gauge, temperature, and soil moisture sensors were connected to a Dynamax SapIP wireless data logger (Figure 1D), which collected data every 15 min and transmitted them via the Dynamax Agrisensors Platinum website (www.agrisensors.net). Voltage signals are converted to millimeter units using a linear factory calibration (Dynamax, Inc., Houston, TX, USA).

2.3. Determining the Effect of Temperature on the Sensor

The strain gauge sensor is temperature-sensitive. This effect was corrected in the experimental data, following [6]. The temperature effect was measured by placing an Invar metal-alloy cylinder between the anvils at mid-strain and exposing it to a range of diurnal sensor temperatures measured by the PRT described above. Invar was chosen because of its very low coefficient of thermal expansion [25], making it a stable target for studies of temperature effects. The relationship between temperature (T) and apparent thickness (S_a) was determined as:

$$S_a = b_0 + b_1 T \tag{1}$$

where b_0 is the intercept (mm) at 0 °C, and b_1 is the slope of the relationship between apparent thickness and temperature. This predicted value represents a thermal error. The error was set to zero at the mean temperature (33.86 °C). These error values were then added to or subtracted from each biological observation, depending on the sensor temperature relative to 33.86 °C. The effect of the temperature correction is presented by displaying diurnal residuals for both corrected and uncorrected data.

2.4. Characterizing Outliers

Repeated spike outliers were characterized by their daily spike range (mm) for spikes associated with and without periodic irrigation. These two conditions and their changes over time (t, days) were explained as:

$$\text{Spike range} = b_0 + b_1 t + b_2 \text{condition} \tag{2}$$

where b_0 is the intercept (mm) when time = 0, b_1 is the slope of the relationship between the spike range and time (t, days), and b_2 is the relative difference between the two conditions.

2.5. Daily Growth

Daily growth was defined as the mean (μ, mm) of each day's observations, of which there are 96, after [26], which were then related to time as:

$$\mu = b_0 + b_1 t \tag{3}$$

where b_0 is the intercept (mm) when time = 0, and b_1 is the slope of the relationship between the mean daily thickness and time (t, days). Data collection using complete daily observations for growth began on 11 July 2025 and ended on 21 July. The total increase in thickness (μ_t) was calculated at the end of the field trial as:

$$\mu_t = \mu_f - \mu_i \tag{4}$$

where f and i are the final and initial mean observations, respectively.

The increase in the mass of the test tuber was estimated by relating the measured mass (379.1 g) on an Ohaus Scout scale to the tuber's single measured thickness, its height (H) as used by [27]. The final tuber height was 57 mm, measured at the center of the anvil locations with a caliper. Both mass and H were measured immediately after harvesting the tuber. Height was related to tuber mass, following the approach of [27] for Irish potatoes. While it would be more accurate to relate an ellipsoidal volume, calculated from all three dimensions, to mass, as in [28], or to use a linear regression incorporating all three measurements, as in [27], this is not feasible here. The other two larger dimensions cannot be measured with the sensor, and they should not be assumed to be proportional to the measured dimension because potato tuber growth and shrinkage are anisotropic, meaning dimensions such as height, length, and width change at different rates. The relationship in [27] was highly significant (r^2 = 0.781) using only H, and was used here as:

$$M = 0.002\ H^{3.006} \tag{5}$$

where M is mass (g), and the exponent was adjusted to match the measured mass of the tuber. This modification likely provides a reasonable approximation for the small growth and diurnal height changes observed in this study. It should be noted that estimating mass using a sensor that measures only one dimension will require either relating existing dimensional and mass data for a specific variety or taking empirical measurements of the dimensions and masses of potato tubers across a full range of sizes.

2.6. Determining Diurnal Thickness Variation and an Estimate of Daily Transpiration as Related to the Mean Estimated Vapor Pressure Deficit

Diurnal thickness variation was distinguished from continuous growth (G) by first fitting a linear regression to the thickness (Th) data as:

$$G = b_0 + b_1 Th. \tag{6}$$

Then residuals (R) were computed as:

$$R = Th - G \tag{7}$$

representing diurnal thickness variation. Residuals were determined for both temperature-corrected and uncorrected data.

The diurnal thickness data can be used to estimate water loss from the tuber and quantify its contribution to the plant's daily transpiration. The daily transpiration (Tr, mL day^{-1}) contribution was estimated by calculating the difference in tuber thickness between the maximum thickness (Th_{max}) in the early morning and the minimum thickness (Th_{min}) at the end of each day. This change was subtracted from the final height and then used in Equation (5) to estimate daily water loss. Given that the Shepody variety is 82% water, the daily percentage of water loss was based on 82% of the final mass (379.1 g), resulting in 310.9 g or mL of H_2O.

Because relative humidity was not measured, the relationship between Tr and the mean estimated vapor pressure deficit (VPD, kPa) was derived from dew-point temperature (T_{dew}) data collected at the Washington State University Pasco NW site, about 8.8 km west of the study site, and from the site's mean air temperature (T_{air}) measured about 70 cm above the ground, just above the canopy. The air temperature sensor (PRT) is located inside the white ABS plastic housing (Figure 1D). The T_{dew} was determined from hourly observations and averaged over the period between Th_{max} and Th_{min} for each of 11 days. The estimated vapor pressure is:

$$VPD = 0.61094\,(\exp(17.625\,T_{air}/243.04 + T_{air}) - \exp(17.625\,T_{dew}/243.04 + T_{dew})) \tag{8}$$

This relationship was modeled using linear regression as:

$$Tr = b_0 + b_1 VPD \tag{9}$$

where b_0 is the intercept when the VPD is 0 kPa, and b_1 is the slope of the relationship between estimated transpiration and the estimated VPD.

2.7. Data Analysis

Data were analyzed using JMP version 18.2.1 software [29]. Outliers were removed using JMP JSL scripting language based on median absolute deviation (24), with a 4-observation rolling window and a threshold consistency scaling factor of 1.4826. Error terms represent 1 standard error of the mean (SEM). Statistical significance was set at $\alpha = 0.05$.

3. Results

3.1. Effect of Temperature on the Sensor

To address the effect of temperature on the sensor, a thermally stable Invar piece [25] was placed at mid-strain between the anvils on the sensor (Figure 1A) and then subjected to a range of temperatures [6]. The effect of temperature on apparent thickness was linear (Equation (1), Figure 2) and highly significant (r^2 = 0.99, p < 0.0001, n = 61), with b_0 = 5.961 ± 0.00257 mm (p < 0.0001) and b_1 = 0.006859 ± 0.00007433 dS_a/dT (p < 0.0001). The range of apparent thickness was 0.14404 mm over 20 °C. After zeroing the error at the mean temperature, the relationship showed b_0 = −0.23224 ± 0.00257 mm (p < 0.0001), with the same b_1 value. The thermal error values ranged from −0.07228 to 0.07176 mm and were subtracted from the tuber thickness data as a function of temperature.

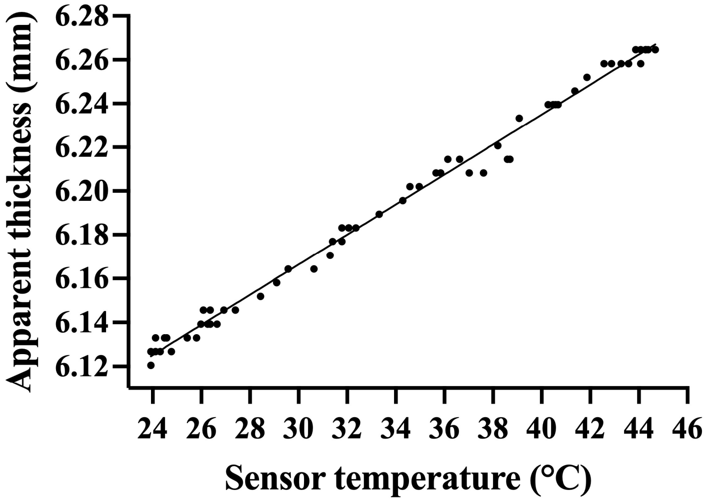

Figure 2. The relationship (Equation (1)) between the apparent thickness (S_a) of a temperature-insensitive Invar bar and sensor temperature.

3.2. Outliers

Outliers were detected repeatedly over 11 days (Figure 3A). The sensor appears to be affected by periodic extraneous noise related to the irrigation process (red, Figure 3B) and by another periodic process (green) unrelated to water. The relationship (Equation (2)) between spike range (mm) for the two irrigation conditions and time was significant (p < 0.0027, r^2 = 0.52, n = 19). The intercept was 0.328 ± 0.0621 (p < 0.0001), and the spike range decreased significantly over time (b_1 = −0.0360 ± 0.0102, p = 0.0027). The effect of the two irrigation conditions was nearly significant (b_2 = −0.0610 ± 0.0295, p = 0.0548), with the least squares mean of the spike range associated with irrigation at 0.196 ± 0.0427 being nearly significantly (p = 0.0548) greater than the spike range not associated with irrigation, which was 0.0737 ± 0.0405.

3.3. Growth

The tuber grew steadily during the observation period (Figure 4A). The linear relationship (Equation (3)), which is highly significant (r^2 = 0.97, p < 0.0001, n = 11), has coefficients of b_0 = −0.0104 ± 0.0284 and b_1 = 0.0761 ± 0.00419. The tuber increased in thickness by 0.80 mm over 11 days. Based on the final measured tuber height of 57 mm, subtracting 0.80 mm yields a final percentage increase in height of 1.4%.

The growth rate was estimated by first predicting the initial mass using Equation (5) with H = 56.2 mm, which yielded 363.7 g. The difference between the final mass of 379.1 g and the predicted initial mass was 15.4 g, yielding an estimated growth rate of 1.4 g day^{-1} and a 4.2% increase in mass over 11 days.

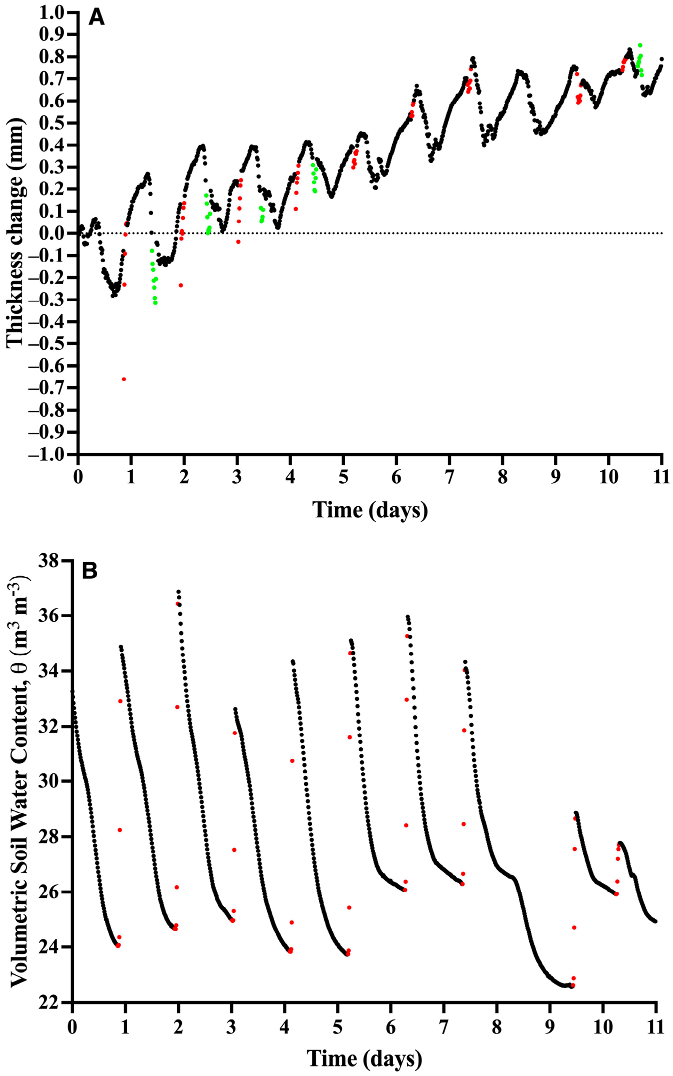

Figure 3. Outliers. (**A**) The temperature-corrected tuber thickness changed from 11 to 21 July. Note the periodic red points, which are aligned with irrigation applications in Figure 3B, and the green points, which were not associated with water. (**B**) The volumetric soil water content at the red points during irrigation corresponded to the red outliers in thickness change in Figure 3A.

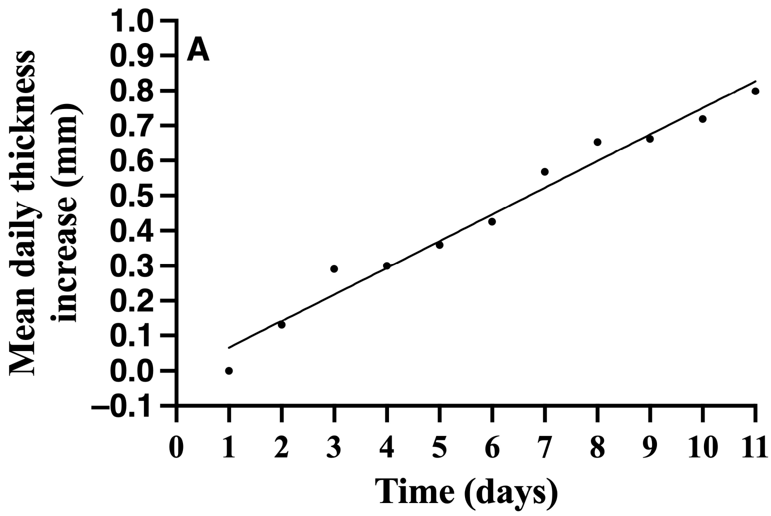

Figure 4. *Cont.*

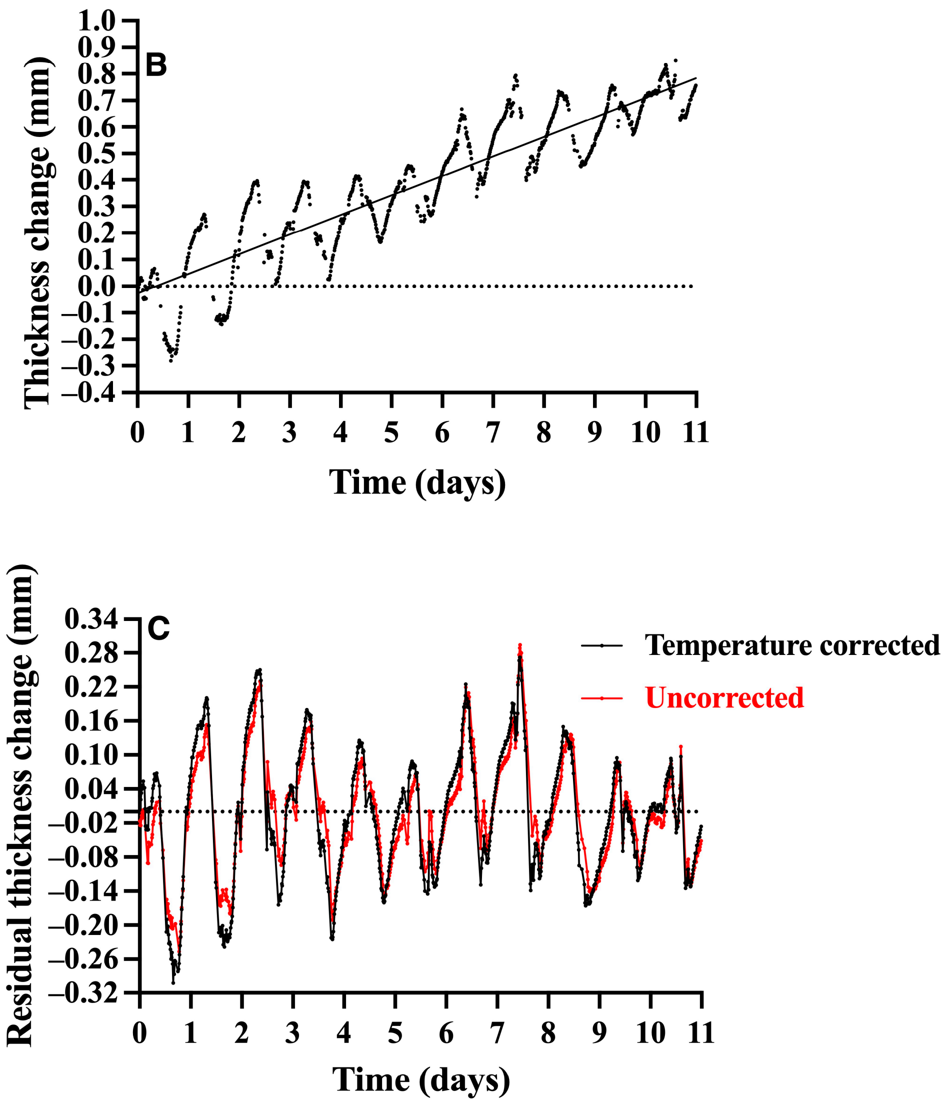

Figure 4. Growth and diurnal residuals. (**A**) The mean daily thickness (height) increases from 11 to 21 July , based on the data in Figure 4B. (**B**) The linear regression fit represents growth. (**C**) Residuals taken from the growth function in Figure 4B with and without temperature correction.

3.4. Diurnal Thickness Variation and an Estimate of Daily Transpiration as Related to the Mean Estimated Vapor Pressure Deficit

Transpiration was estimated by separating growth from diurnal variation. This was done by first predicting continuous growth using Equation (6) (Figure 4B; $b_0 = -0.0273 \pm 0.00778$, $b_1 = 0.0738 \pm 0.00120$, $n = 904$, $r^2 = 0.808$, $p < 0.0001$). The resulting residuals (Equation (7)) are considered representative of diurnal variations in thickness associated with water status (Figure 4C). Diurnal variation ranged from 0.216 to 0.439 mm for temperature-corrected values and from 0.177 to 0.392 for uncorrected values (Figure 4C).

The estimated contribution of water for whole plant transpiration, based on temperature-corrected residuals, from the test tuber ranged from a maximum of 9.1 mL or 2.9% of the full 310.9 mL of water stored in the tuber to a minimum of 4.7 mL or 1.5% (Figure 5A). The mean air temperature ranged from 40.8 °C to 26.5 °C on the last day. The relationship with the mean daily vapor pressure deficit was highly significant ($p = 0.0009$, $r^2 = 0.72$), with $b_0 = 2.25 \pm 1.02$ and $b_1 = 1.15 \pm 0.234$ (Figure 5C). For a comparison with data without temperature correction, the relationship with the mean daily vapor pressure deficit was also highly significant ($p = 0.0009$, $r^2 = 0.72$), with $b_0 = 2.47 \pm 0.97$ and $b_1 = 1.10 \pm 0.227$. Neither parameter value differs significantly.

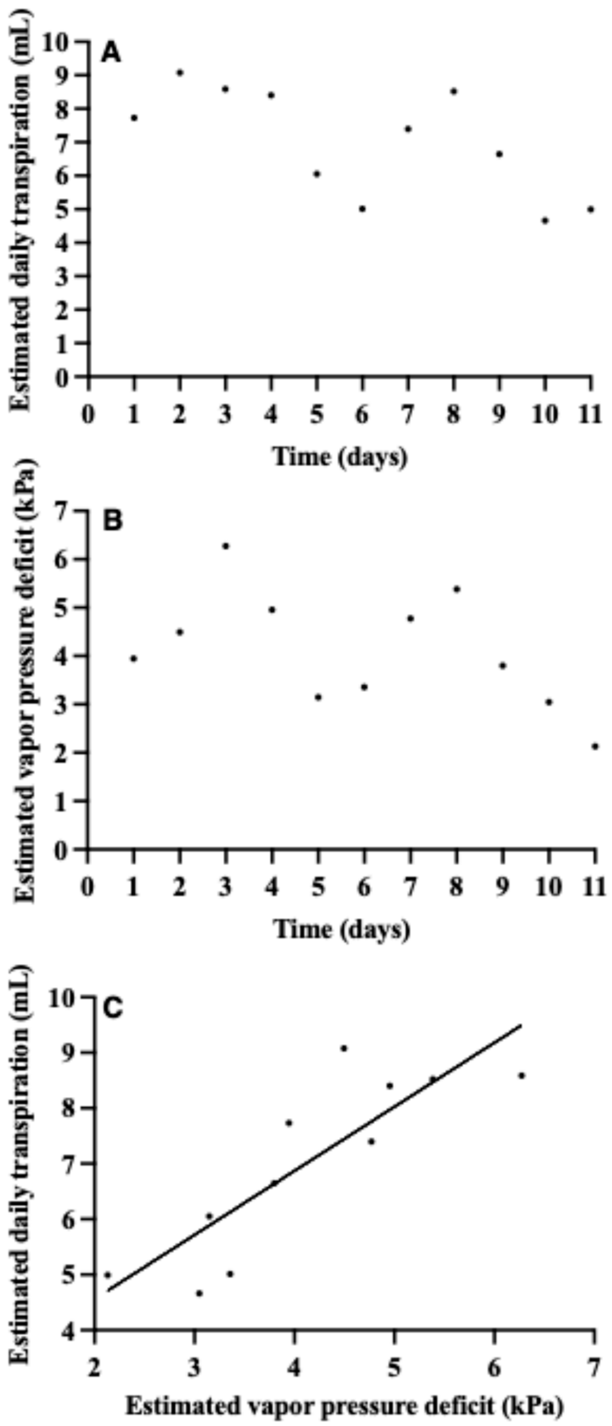

Figure 5. Estimated daily transpiration. (**A**) The contribution to the daily rate by the test tuber. (**B**) Mean estimated vapor pressure deficit during the period of daily transpiration in Figure 5A. (**C**) The relationship between the estimated water loss or contribution to daily whole-plant transpiration from the test tuber and the estimated vapor pressure deficit derived from dew point records collected 8.8 km west of the site.

4. Discussion

The main goals of this study were to determine whether the sensor could reliably measure underground tuber growth in real time and to estimate the tuber's contribution to transpiration. These goals appear to have been met, as evidenced by consistent daily patterns, a 0.80 mm increase over 11 days, and a positive relationship between VPD and the tuber's water loss. The sensor is the first to do so for underground tubers in an agricultural setting.

4.1. Effect of Temperature on the Sensor

The sensor used here, along with other commonly used sensors, is temperature-sensitive [7,30], which can impair the ability to relate diurnal variation to water status [31]. With 20 °C changes, thermal noise is less than 10 µm for a potentiometer [32], ranges from 17 to 27 µm for LVDTs [30], and is 50 µm for the smaller DEX20 strain-gauge sensor (Dynamax, Inc., Houston, TX, USA) on olive fruit [11]. This is much smaller than the 144 µm variation observed with the larger DEX100 strain-gauge sensor, underscoring the need to consider temperature effects when diurnal thickness changes range from 216 to 439 µm, a difference of 223 µm that results in a range of estimated water loss of 4.6 mL. Even though the effect of temperature on the data was small, given that the difference without temperature correction was only 215 µm, which results in a range of estimated water loss of only 4.4 mL, this effect may be of importance with a greater range of temperatures, which may be able to reduce high signal-to-noise ratios that can impair the ability to relate diurnal variation to water status [33].

4.2. Outliers

Outliers are a problem with strain-gauge data and must be removed to draw conclusions about growth and water status [31]. In this study, periodic, mostly negative spikes occurred when the pivot-irrigation system passed over the sensor. These spikes lasted up to 2 h and were larger at the beginning of the trial. Because some spikes were not linked to water application, they may have been caused by other sources of electromagnetic interference [33,34]. Such interference could originate from the motors of nearby equipment. It is also possible that the sensor detected soil vibrations [35] associated with the pivot irrigation system. Because the spike range was higher during water application than for other outliers, there may have been an additive effect of water on the sensor. The reduction in spike range over time suggests that these environmental factors may be temporary. The sensor behaved similarly to those on apples [6], except for the repeated outliers. The sensor used in the orchard was not repeatedly exposed to electromagnetic interference, showing only three spiked outliers on stems and one on an apple over 15 d [6]. Removing spikes from strain gauge data was easily done using a moving median data filter with a threshold [26].

4.3. Growth and Yield Estimation

The tuber grew at 1.4 g day^{-1}, comparable to the 1.36 g day^{-1} growth rate of a Honeycrisp apple under similar conditions [36]. Both were well-watered. In a controlled greenhouse, the Julinka potato cultivar grew at about 4 g day^{-1} during the final stage of potato growth [37]. There appears to be little other information on individual tuber daily growth rates under field conditions.

Yield estimation is crucial for all crops and is relatively simple for above-ground crops. For example, modeled apple fruit diameters improve early yield predictions [38,39], and fruit growth sensors provide reliable yield forecasts up to 8 days after data collection [39]. However, predicting yield for below-ground crops is much more difficult. As a result, models link yield to observable, correlated traits. Recent reviews [40,41] of potato yield prediction note that these efforts have been ongoing, with varying success. This is partly because modeling tuber growth using only correlated predictors is inherently less accurate than models based on direct measurements of the target. Current methods, such as machine learning, improve accuracy but require large datasets and are difficult to implement at the individual-farm level [40,42]. Belowground crop models are limited by the lack of real-time tuber growth data, which could simplify and improve model logic [42]. The positive results here suggest that measuring below-ground growth in real time, as easily as for above-ground crops, will streamline yield prediction for potatoes and, likely, other below-ground crops.

https://doi.org/10.3390/agronomy16181803

The ability to monitor tuber growth in real time enables estimation of daily increases in potato yield. While using a single potato to estimate yield primarily serves as a demonstration, it is now possible—with sufficient sensors and knowledge of size distribution for a specific cultivar—to provide a reasonable field estimate. For example, the tuber grew 4.2% over 11 days. Based on this, and the average yield of 6.95 kg m^{-2} (31 tons $acre^{-1}$) in the Columbia Basin in 2024 [43], the yield 11 days before harvest would have been around 6.66 kg m^{-2} (29.71 tons $acre^{-1}$); thus, the yield increased by 0.289 kg m^{-2} (1.29 tons per acre) at a rate of 0.0263 kg day^{-1} (0.117 tons day^{-1}). At a price of \$10.40 per 45.36 kg (100-pound hundredweight (CWT)) [43], or \$0.229 kg^{-1} (\$208 ton^{-1}), a 0.405 km^2 (100-acre) field could generate \$2434 day^{-1} during the 11 days before harvest. The sensor's timely information will help managers balance daily maintenance costs against the estimated increase in value to optimize harvest timing.

The ability to measure tuber growth in real time also enables Proportional-Integral-Derivative (PID) fertigation control logic, in which tuber size and growth rate serve as control targets. Such control logic may be similar to that used for fruit growth, which is directly related to fruit yield and has demonstrated positive results for irrigation scheduling [44].

4.4. Diurnal Thickness Variation and an Estimate of Daily Transpiration as Related to the Mean Estimated Vapor Pressure Deficit

For water storage dynamics, the maximum diurnal variation of 0.44 mm is similar to that of cucumbers (0.40 mm) [10], tomatoes (0.45 mm) [41], olives (0.55 mm) [11], and apples (0.7 mm) [36]. This suggests that the sensor operating underground is much like sensors measuring diurnal variation in above-ground crops. This technological advancement will now allow exploration of the role of tuber water storage in water budget models and its contribution to transpiration under field conditions.

Potato tuber water storage may be significant because tubers can account for 78% of total plant biomass [45], with 82% of the Shepody tuber biomass being water [20]. Because they do not exchange water with their environment, they supply water to the shoot [3], as do olives [11]. The maximum daily percentage water loss in this study was 2.9% in about 18-week-old plants, and while experimental conditions differed, it appears to be less than the 10% daily water loss in 6-week-old plants [2], largely supporting observations that transpiration decreases significantly as plants senesce [46].

The daily estimated contribution to whole-plant transpiration rates was positively correlated with the estimated VPD, supporting the observation that transpiration rates increase with increasing VPD for well-watered plants [19,20]. It appears that the sensor can be used to estimate transpiration rates similar to how dendrometers are used for above-ground crops [15–17]. This approach and regression should be considered exploratory because the dew point above the canopy will differ from observations 8.8 km distant, and the reported air temperature is not well-ventilated. In addition, plant transpiration potential may also decrease as the plants senesce.

The contribution of stored tuber water to daily transpiration can also be compared with irrigation rates. Assuming a single tuber represents the others in a field, a 2.9% loss of water would be calculated as 6.95 kg m^{-2} (31 tons $acre^{-1}$) $\times$ 0.82 $\times$ 0.029, resulting in 0.1653 kg m^{-2}) (0.74 tons $acre^{-1}$). This amount is only about 2.6% of the typical application rate at the season's end, which is 6.35 mm or 6.35 m^{-3} water m^{-2}. The contribution of stored tuber water can also be compared with an average crop evapotranspiration rate of 3.42 mm day^{-1} for potatoes at the end of the season in the Columbia Basin [47]. In that context, the contribution from tubers would be approximately 0.165 mm day^{-1}, or 4.8% of the crop's evapotranspiration rate. While this contribution rate appears small, it may be larger in younger plants and could be useful for refining water budgets for potatoes.

Potential applications of the technology also include tracking hydration levels. This is crucial for reducing damage from blackspot [48,49] and shatter bruise [49]. These sources note that blackspot damage is high when tubers are dehydrated and shatter damage is high when tubers are crisp or very turgid. Determining the optimal harvest time to minimize damage is challenging because tuber weight decreases when roots are pruned and increases when plant tops are removed [48]. Harvesting when water content is high can boost yield for the producer but may harm the processor [48]. A tuber sensor can provide size and an estimate of water content in real time, likely improving the ability to minimize damage and maximize yield.

Although the current sensor worked on a large tuber at the end of the growing season, it is important to test the sensor or similar sensors over a longer period. Smaller tubers can be accommodated by designing smaller anvils and using a narrower pipe. A narrower, longer pipe will also reduce light and greening, as was observed at a low level here. Greening does not appear to affect tuber growth rates [50] and likely is not an issue. There is potential that stiff sensors can affect the morphology of a fruit or tuber. This is mitigated by the DEX100 sensor, which has a flexible band and uses a large-surface-area anvil to reduce pressure on the growing surface [6]. In addition, the sensor has to be periodically reset to a lower pressure to avoid damaging the strain gauges. While the current study lasted only 11 days, there did not appear to be any surface deformation associated with the sensor.

5. Conclusions

The sensor, or its modifications, will likely work across all belowground food crops and contribute to precision agriculture. This new capacity to measure tuber size in real time under field conditions will help improve our understanding of the relationships among growth, water status, daily transpiration, and external factors. This may enable more precise control of inputs at a much higher temporal resolution than current methods for belowground crops. This should improve quality and yield while reducing inputs, saving water, nutrients, and power. The sensor, or its modifications, can likely also measure relatively shallow rhizome and thick-root growth, as well as their diurnal variation.

Funding: This research received no external funding.

Data Availability Statement: Supporting data and coding are available from the corresponding author on request or Dryad (DOI: 10.5061/dryad.7d7wm389q).

Acknowledgments: M.G. van Bavel is thanked for his advice on sensor use. Field and technical assistance from E. Mendoza and N. Sheshunov are appreciated. Suggestions by J. Blauer and A. Schreiber that enhanced the manuscript are appreciated. Comments on the manuscript by E. Mendoza and M. Rubalcava are acknowledged. The potato field for this research was provided by C. Sullivan.

Conflicts of Interest: Author Steven Otto Link was employed by the company Link Agricultural Technologies LLC., West Richland, USA.

Abbreviations

The following abbreviations are used in this manuscript:

MRI	Magnetic resonance imaging
LVDT	Linear variable differential transformer
VPD	Vapor pressure deficit
PRT	Platinum resistance thermometer
JSL	JMP Scripting Language
ABS	Acrylonitrile Butadiene Styrene

References

1. Waldburger, T.; Anken, T.; Cockburn, M.; Walter, A.; Hatt, M.; Chiang, C.; Nasser, H. Automated irrigation of apple trees based on dendrometer sensors. *Agric. Water Manag.* **2025**, *311*, 109398. [CrossRef]
2. Huntenburg, K.; Pflugfelder, D.; Koller, R.; Dodd, I.C.; van Dusschoten, D. Diurnal water fluxes and growth patterns in potato tubers under drought stress. *Plant Soil* **2025**, *507*, 269–282. [CrossRef]
3. Stark, J.C.; Halderson, J.L. Measurement of diurnal changes in potato tuber growth. *Am. Potato J.* **1987**, *64*, 245–248. [CrossRef]
4. Pérez-Torres, E.; Kirchgessner, N.; Pfeifer, J.; Walter, A. Assessing potato tuber diel growth by means of X-ray computed tomography. *Plant Cell Environ.* **2015**, *33*, 2318–2326. [CrossRef] [PubMed]
5. Shimazu, M.; Shibata, Y.; Araki, H.; Kataoka, T.; Okamoto, H. Measurement of dilation of root crops. In Proceedings of the XVIIth World Congress of the International Commission of Agricultural and Biosystems Engineering (CIGR, 2010), Quebec, QC, Canada, 13–17 June 2010; pp. 1–10.
6. Link, S.O.; Thiede, M.E.; van Bavel, M.G. An improved strain-gauge device for continuous field measurement of stem and fruit diameter. *J. Exp. Bot.* **1998**, *49*, 1583–1587. [CrossRef]
7. Link, S.O.; Drake, S.R.; Thiede, M.E. Prediction of apple firmness from mass loss and shrinkage. *J. Food Qual.* **2004**, *27*, 13–26. [CrossRef]
8. Swaef, T.D.; Steppe, K. Linking stem diameter variations to sap flow, turgor and water potential in tomato. *Funct. Plant Biol.* **2010**, *37*, 429–438. [CrossRef]
9. Zucchini, M.; Khosravi, A.; Giorgi, V.; Mancini, A.; Neri, D. Is there daily growth hysteresis versus vapor pressure deficit in cherry fruit? *Horticulturae* **2021**, *7*, 131. [CrossRef]
10. Ruijiang, W.; Wang, X.; Zhu, H. Dynamic changes of transverse diameter of cucumber fruit in solar greenhouse based on no damage monitoring. In Proceedings of the 9th International Conference on Computer and Computing Technologies in Agriculture (CCTA, 2015), Beijing, China, 27–30 September 2015; pp. 458–469. [CrossRef]
11. Khosravi, A.; Zucchini, M.; Giorgi, V.; Mancini, A.; Neri, D. Continuous monitoring of olive fruit growth by automatic extensimeter in response to vapor pressure deficit from pit hardening to harvest. *Horticulturae* **2021**, *7*, 349. [CrossRef]
12. Gallardo, M.; Thompson, R.B.; Valdez, L.C.; Fernández, M.D. Use of stem diameter variations to detect plant water stress in tomato. *Irrig. Sci.* **2006**, *24*, 241–255. [CrossRef]
13. Nortes, P.A.; Pérez-Pastor, A.; Egea, G.; Conejero, W.; Domingo, R. Comparison of changes in stem diameter and water potential values for detecting water stress in young almond trees. *Agric. Water Manag.* **2005**, *77*, 296–307. [CrossRef]
14. Scalisi, A.; Bresilla, K.; Grilo, F.S. Continuous determination of fruit tree water-status by plant-based sensors. *Italus Hortus* **2017**, *24*, 39–50. [CrossRef]
15. De Schepper, V.; Van Dusschoten, D.; Copini, P.; Jahnke, S.; Steppe, K. MRI links stem water content to stem diameter variations in transpiring trees. *J. Exp. Bot.* **2012**, *63*, 2645–2653. [CrossRef] [PubMed]
16. Simonneau, T.; Habib, R.; Goutouly, J.-P.; Huguet, J.-G. Diurnal changes in stem diameter depend upon variations in water content: Direct evidence in peach trees. *J. Exp. Bot.* **1993**, *44*, 615–621. [CrossRef]
17. Sperling, O.; Kamai, T.; Gardi, I.A.; Zwieniecki, M.; Marino, G. Modeling tree responses to soil water variability guides irrigation to account for soil winter reserves. *Vadose Zone J.* **2025**, *24*, e20385. [CrossRef]
18. Geremew, E.B.; Steyn, J.M.; Annandale, J.G. Evaluation of growth performance and dry matter partitioning of four processing potato (*Solanum tuberosum*) cultivars. *N. Z. J. Crop Hortic. Sci.* **2007**, *35*, 385–393. [CrossRef]
19. Ribeiro, R.V.; Machado, E.C.; Santos, M.G.; Oliveira, R.F. Photosynthesis and water relations of well-watered orange plants as affected by winter and summer conditions. *Photosynthetica* **2009**, *47*, 215–222. [CrossRef]
20. Zhang, P.; Yang, X.; Manevski, K.; Li, S.; Wei, Z.; Andersen, M.N.; Liu, F. Physiological and growth responses of potato (*Solanum tuberosum* L.) to air temperature and relative humidity under soil water deficits. *Plants* **2022**, *11*, 1126. [CrossRef] [PubMed]
21. Adamchuk, V.I.; Morgan, M.T.; Sumali, H. Application of a strain gauge array to estimate soil mechanical impedance on–the–go. *Trans. ASAE* **2001**, *44*, 1377–1383. [CrossRef]
22. Kahrobaee, S.; Vuran, M.C. Vibration energy harvesting for wireless underground sensor networks. In Proceedings of the 2013 IEEE International Conference on Communications (ICC, 2013), Budapest, Hungary, 9–13 June 2013; pp. 1543–1548.
23. Hoffmann, K. *An Introduction to Stress Analysis and Transducer Design Using Strain Gauges*; HBM Test and Measurement: Darmstadt, Germany, 2012.
24. Hampel, F.R. The influence curve and its role in robust estimation. *J. Am. Stat. Assoc.* **1974**, *69*, 383–393. [CrossRef]
25. Katerji, N.; Tardieu, F.; Bethenod, O.; Quentin, P. Behavior of maize stem diameter during drying cycles: Comparison of two methods for detecting water stress. *Crop Sci.* **1994**, *34*, 165–169. [CrossRef]
26. Oberhuber, W.; Gruber, A.; Kofler, W.; Swidrak, I. Radial stem growth in response to microclimate and soil moisture in a drought-prone mixed coniferous forest at an inner Alpine site. *Eur. J. For. Res.* **2014**, *133*, 467–479. [CrossRef] [PubMed]
27. Oyefeso, B.O.; Raji, A.O. Estimating mass and volume of Nigerian grown sweet and Irish potato tubers using their geometrical attributes. *Adeleke Univ. J. Eng. Technol.* **2018**, *1*, 123–130.

28. Pitts, J.; Hyde, G.M.; Cavalieri, R.P. Modeling potato tuber mass with tuber dimensions. *Trans. ASAE* **1987**, *30*, 1154–1159. [CrossRef]
29. JMP Statistical Discovery LLC. *JMP®*; JMP Statistical Discovery LLC.: Cary, NC, USA, 2025.
30. Erasmus, C.S.; Drew, D.; Booysen, M.J. A low-cost wireless dendrometer and digital twin for precision forestry applications. *Measurement* **2026**, *276*, 121442. [CrossRef]
31. Francini, S.; Cocozza, C.; Hölttä, T.; Lintunen, A.; Paljakka, T.; Chirici, G.; Traversi, M.L.; Giovannelli, A. A temporal segmentation approach for dendrometers signal-to-noise discrimination. *Comput. Electron. Agric.* **2023**, *210*, 107925. [CrossRef]
32. Morandi, B.; Manfrini, L.; Zibordi, M.; Noferini, M.; Fiori, G.; Grappadelli, L.C. A low-cost device for accurate and continuous measurements of fruit diameter. *HortScience* **2007**, *42*, 1380–1382. [CrossRef]
33. Ott, H.W. *Noise Reduction Techniques in Electronic Systems*, 2nd ed.; John Wiley &Sons, Inc.: New York, NY, USA, 1988.
34. Liu, Q.; Ding, W.; Zhou, H.; Han, R.; Wu, J.; Jing, Y.; Qiu, A. A novel strain measurement system in strong electromagnetic field. *IEEE Trans. Plasma Sci.* **2015**, *43*, 3562–3567. [CrossRef]
35. Ágoston, K. Vibration detection of the electrical motors using strain gauges. *Procedia Technol.* **2016**, *22*, 767–772. [CrossRef]
36. Blanco, V.; Kalcsits, L. Relating microtensiometer-based trunk water potential with sap flow, canopy temperature, and trunk and fruit diameter variations for irrigated 'Honeycrisp'apple. *Front. Plant Sci.* **2024**, *15*, 1393028. [CrossRef] [PubMed]
37. Jama-Rodzenska, A.; Janik, G.; Walczak, A.; Adamczewska-Sowinska, K.; Sowinski, J. Tuber yield and water efficiency of early potato varieties (*Solanum tuberosum* L.) cultivated under various irrigation levels. *Sci. Rep.* **2021**, *11*, 19121. [CrossRef] [PubMed]
38. Stajnko, D.; Črtomir, R.; Pavlovič, M.; Beber, M.; Zadravec, P. Modeling of 'Gala'apple fruits diameter for improving the accuracy of early yield prediction. *Sci. Hortic.* **2013**, *160*, 306–312. [CrossRef]
39. Najdenovska, E.; Carvalho, C.C.; Dunkel, T.; Whittaker, R.; Monney, P.; Dutoit, F.; Raileanu, L.E. LSTM-based prediction of apple fruit growth using past diameter and climatic condition data. In Proceedings of the 2025 International Conference on Artificial Intelligence, Computer, Data Sciences and Applications (ACDSA IEEE, 2025), Antalya, Türkiye, 7–9 August 2025; pp. 1–6.
40. Piekutowska, M.; Gniewko, N. Review of methods and models for potato yield prediction. *Agriculture* **2025**, *15*, 367. [CrossRef]
41. Dunkel, T.; Najdenovska, E.; Dutoit, F.; Whittaker, R.; Raileanu, L.E.; Camps, C. Novel fruit growers' advisory system using connected fruit dendrometer, micro-climate data and machine learning algorithms. In Proceedings of the International Symposium on New Technologies for Sustainable Greenhouse Systems (GreenSys, 2023), Cancún, Mexico, 22–27 October 2023; pp. 333–340.
42. Lin, Y.; Li, S.; Duan, S.; Ye, Y.; Li, B.; Li, G.; Lyv, D.; Jin, L.; Bian, C.; Liu, J. Methodological evolution of potato yield prediction: A comprehensive review. *Front. Plant Sci.* **2023**, *14*, 1214006. [CrossRef] [PubMed]
43. USDA. *2024 Washington State Agricultural Review*; USDA: Washington, DC, USA, 2025. Available online: https://linkagriculturaltechnologiesllc.com/references/ (accessed on 24 August 2026).
44. Fernandes, R.D.M.; Cuevas, M.V.; Diaz-Espejo, A.; Hernandez-Santana, V. Effects of water stress on fruit growth and water relations between fruits and leaves in a hedgerow olive orchard. *Agric. Water Manag.* **2018**, *210*, 32–40. [CrossRef]
45. Fleisher, D.H.; Timlin, D.J.; Yang, Y.; Reddy, V.R. Simulation of potato gas exchange rates using SPUDSIM. *Agric. For. Meteorol.* **2010**, *150*, 432–442. [CrossRef]
46. Nelson, S.H.; Hwang, K.E. Water usage by potato plants at different stages of growth. *Am. Potato J.* **1975**, *52*, 331–339. [CrossRef]
47. Gonzalez, F.T.; Pavek, M.J.; Holden, Z.J.; Garza, R. Evaluating potato evapotranspiration and crop coefficients in the Columbia Basin of Washington state. *Agric. Water Manag.* **2023**, *286*, 108371. [CrossRef]
48. Kunkel, R.; Gardner, W.H. Potato tuber hydration and its effect on blackspot of Russet Burbank potatoes in the Columbia Basin of Washington. *Am. Potato J.* **1965**, *42*, 109–124. [CrossRef]
49. Hiller, L.K.; Pelter, G.Q. Conditioning Potatoes for Harvest. In Proceedings of the 14th Annual Washington State Potato Conference and Trade Fair, Moses Lake, WA, USA, 4–6 February 1975.
50. Tanios, S.; Eyles, A.; Tegg, R.; Wilson, C. Potato tuber greening: A review of predisposing factors, management and future challenges. *Am. J. Potato Res.* **2018**, *95*, 248–257. [CrossRef]